Polarization-controlled microgroove arrays induced by femtosecond laser pulses

Erik M. Garcell[1] and Chunlei Guo[1,2,a)]
[1]*The Institute of Optics, University of Rochester, Rochester, New York 14627, USA*
[2]*Changchun Institute of Optics, Fine Mechanics, and Physics, Changchun 130033, China*

(Received 8 March 2018; accepted 11 May 2018; published online 4 June 2018)

Using pulsed femtosecond laser irradiation, we demonstrate the creation of an array of microgrooves within a single laser spot on metals. The orientation of these grooves is not limited to being parallel to the plane of the laser beam's propagation but can orient at any angle up to 30° from parallel. We control the orientation of the microgrooves by proportionally varying the laser's polarization. Polarization, angle of incidence, and structural evolution dynamics have been thoroughly studied to help us understand this phenomenon. Our studies suggest that the formation of angled microgroove arrays is due to a feedback effect occurring between defect-focused ablation and polarization-dependent laser-induced periodic surface structures. https://doi.org/10.1063/1.5028197

I. INTRODUCTION

Laser-ablated microgrooves have long been studied due to their numerous applications in fields such as microfluidics,[1,2] microelectromechanical applications,[3] biomimicry,[4] and other biological systems.[5,6] Femtosecond-pulsed lasers are particularly useful for creating microgroove formation due to their relatively small heat affected zone, which allows for more precise drilling for materials' surfaces when compared to longer pulsed lasers.[7,8] The precision of femtosecond laser systems, along with their increased commercial availability, has made them favored tools for microfabrication applications.[9–11]

In general, microgrooves formed via laser ablation are created parallel to the plane of the laser beam propagation,[12–14] as is the case in standard laser drilling.[15–17] Using pulsed-femtosecond laser irradiation, many different structures can be produced, such as laser-induced periodic surface structures (LIPSSs).[18–21] In this work, using femtosecond laser irradiation, we observe the formation of extensive microgrooves covered by LIPSSs. Additionally, we find that the orientation of these microgrooves can be controlled by varying only the incident laser beam's polarization.

Our technique is a single-step, non-scanning method for the formation of microgroove arrays with variable orientation. The microgrooves studied form with LIPSSs on and around the formed grooves but are significantly larger than LIPSSs (Fig. 1). By irradiating copper (Cu) at large incidence angles, we create an array of roughly 10 μm wide microgrooves within a single laser spot. By varying the incident laser beam's polarization, the orientation of these grooves is controllable between 0° and 30° relative to the plane of the laser beam's propagation. We find that LIPSSs forming on and around the microgrooves can either enhance or inhibit microgroove formation and that a feedback mechanism between defect focused ablation and polarization dependent LIPSSs is the cause of the angled microgroove formation.

II. METHODS

All experiments were carried out using a pulsed Ti-sapphire femtosecond laser system that generates 50 fs linearly polarized pulses operating at a repetition rate of 1 kHz at a central wavelength of 800 nm. The laser beam polarization was varied using a half wave plate. The sample materials used in these experiments were 1 mm polished foils of Cu. The number of pulses was selected using an electromechanical shutter. All experiments were performed in air. The surface structures of the irradiated samples were studied using a scanning electron microscope (SEM) and a UV laser-scanning confocal microscope (UV-LSCM). All images shown were irradiated with the laser beam traveling towards the right-hand side of the image.

III. RESULTS AND DISCUSSION

A. Polarization dependence

Figure 2 is a representative image of the angled microgrooves we have studied. The figure shows a single laser

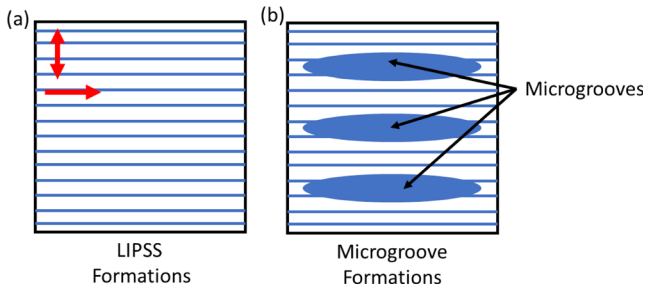

FIG. 1. Illustration of (a) LIPSSs and (b) LIPSS covered microgroove formation. The double headed arrow in (a) represents the laser beam's polarization, while the single headed arrow represents the laser beam's propagating direction.

a)guo@optics.rochester.edu

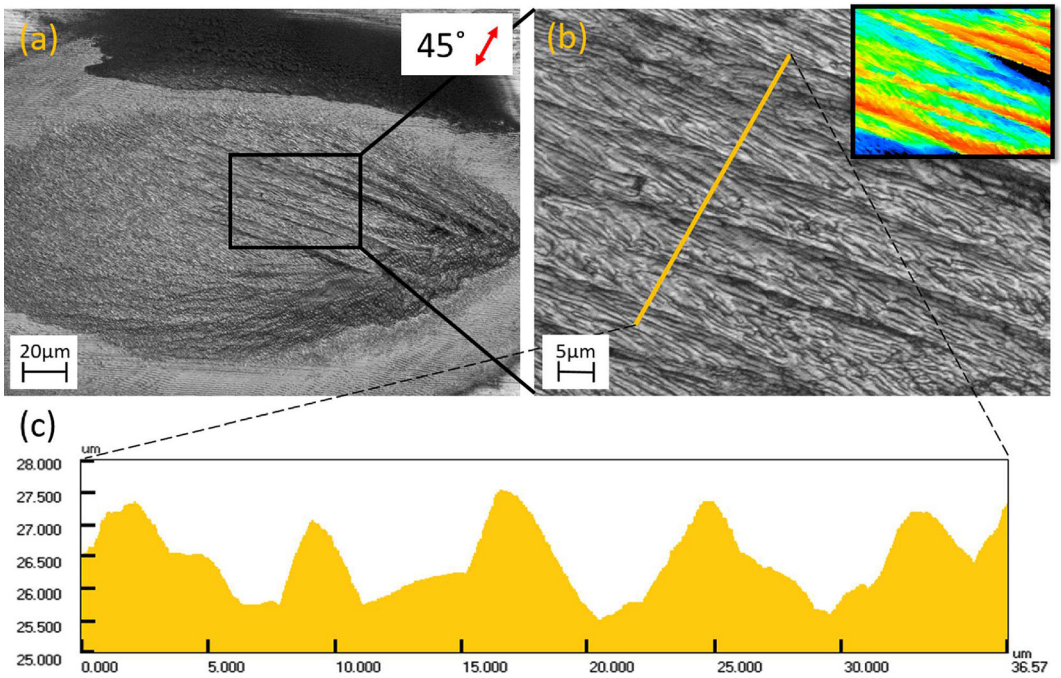

FIG. 2. SEM images of typical grooves formed on the Cu surface with an incident polarization of 45°, irradiated at a 50° incident angle, with 15 000 pulses at an absorbed single pulse fluence of 5.48 mJ/cm^2. (a) Image of the entire area irradiated by the laser beam; the arrow illustrates the polarization direction of the laser. (b) Zoomed in image of microgrooves formed within the irradiated area; the inset figure in the top right is a height map of the image. (c) Surface profile for the line shown in image (b).

spot on a Cu surface with an array of grooves drilled along the material's surface, oriented at an angle 20° from the plane of the laser beam's propagation. Grooves, for the purpose of this paper, refer to any long and continuous ablated region having a depth greater than the immediate surrounding area, which results in a trough-like structure with two sidewalls defining its borders. We can see that these grooves form with saw toothed profiles in Fig. 2(c). The structures shown in Fig. 2 were formed by irradiating a Cu surface with 15 000 pulses at a 50° incident angle. To form grooves without translating or altering the orientation of the laser beam, a large incident angle must be employed. When irradiating at a steep incident angle, we observe that varying the laser's polarization biases the orientation of the grooves formed. To study the dependence of polarization on the formation of the microgroove arrays, we first varied the laser's polarization without changing the laser's orientation.

The polarization component in the surface of the sample was varied from 0 degrees (p-polarized) to 90° (s-polarized), in 5-degree increments. For each polarization, data were taken at three pulse train values: 1000, 5000, and 15 000, using an absorbed single pulse fluence of 5.48 mJ/cm^2, at a laser incident angle of 50°. Constant fluence was achieved in our experimental sets, as polarization and incident angles are changed, by varying the incident laser's power in accordance with the change in material absorption as governed by the Fresnel equations,[22] and accounting for the laser beam's change in the cross sectional area upon the sample's surface. Data are reported using absorbed fluence values calculated with a refractive index of 6.12×10^{-2} and an extinction coefficient of 5.13.[23]

For all polarizations, irradiation with a pulse train of 1k results in LIPSSs forming on the material's surface [Figs. 3(a)–3(d)]. The generally accepted means by which these structures are formed is by the interference of incident laser light with surface scattered electromagnetic waves, causing periodic modulation of the laser's deposited energy, resulting in inhomogeneous ablation of the material.[24–26] Typically, at normal incidence, these ripple-like formation are oriented perpendicular to the incident laser's polarization and have a period proportional to the laser's wavelength.[26–28]

At 5000 and 15 000 pulses, faint angled surface structures covered in LIPSSs are observed on the outer edges of the irradiated area for polarizations between 0 and 20° [Fig. 3(e)]. As polarization is swept towards 90°, these structures become more defined and grow in length. At 20° polarization, these surface structures become clearly defined and form orderly straight lines, having an orientation 30° off from the plane of the laser beam's propagating direction. When packed closely together, these ordered and LIPSS covered structures represent a series of hierarchical microgrooves running along the material's surface. As polarization is swept towards s-polarization, the orientation of these grooves changes, becoming more parallel to the plane of the laser beam's propagation; the orientation of the grooves trends in the same manner as the LIPSSs formed at lower pulse numbers but does not match their orientation [Figs. 3(f)–3(h)]. Note that the orientation of the laser has not changed.

LIPSSs forming on the microgroove structures also change orientation. The change in orientation of these LIPSSs is believed to be the result of a change in the angle of effective polarization on the sidewalls of the underlying ablated grooves due to an altered geometric projection of the laser's polarization. Interestingly, for

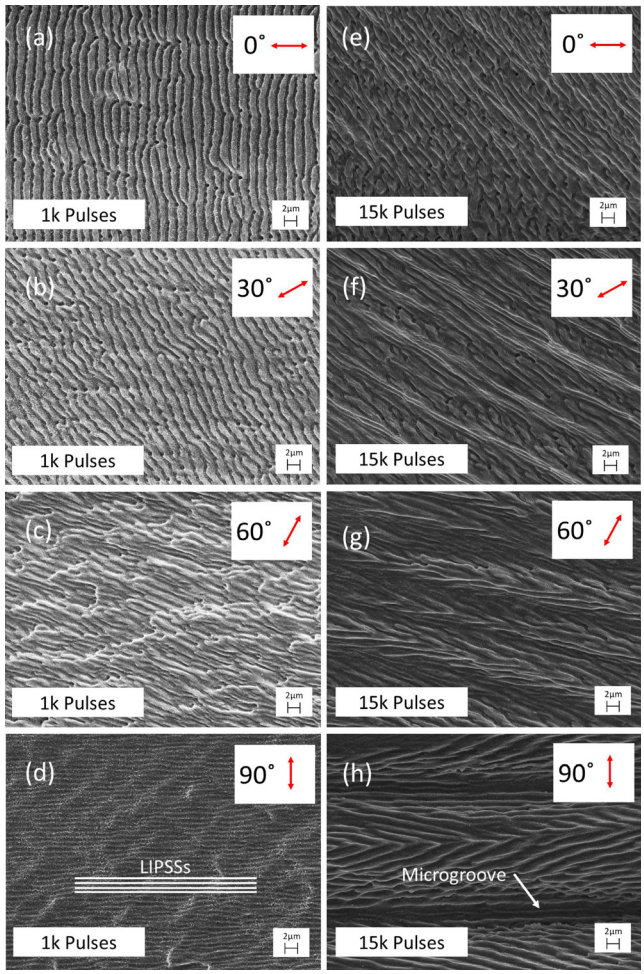

FIG. 3. SEM images illustrating the changing orientation of both LIPSSs and groove formation as the surface component of the laser's polarization is altered. (a)–(d) and (e)–(h) show the changing orientation of LIPSSs and laser drilled grooves, respectively. For comparison, the solid lines in figure (d) mark LIPSS, while the arrow in figure (h) identifies a microgroove.

polarizations between 55° and 90°, the LIPSSs forming along the walls of grooves orient themselves so as to resemble v-shaped structures.

The dependence of the groove's orientation at 15 000 pulses vs the surface component of the laser beam's polarization is plotted in Fig. 4, with reference to the orientation of the LIPSSs formed with 1k pulses without groove formation. Fitting these data presented in Fig. 4 to a linear function, we find that $\theta = -\delta + 87°$ and $\theta' = -0.47\delta + 41°$, where δ, θ, and θ' represent the laser's polarization, LIPSS orientation, and groove orientation, respectively. For the same polarization, groove orientation is found to form nearly at the bisectrix between LIPSS orientation and the plane of the laser beam's propagation. In addition to changing microgroove orientation, as polarization is traversed, the grooves formed also become more defined and grow in length as polarization approaches s-polarization. For pulse trains of 15 000, these grooves have widths of between 8 and 12 μm and depths of between 2 and 6 μm. The width and depth of these structures vary little between the differing polarization conditions.

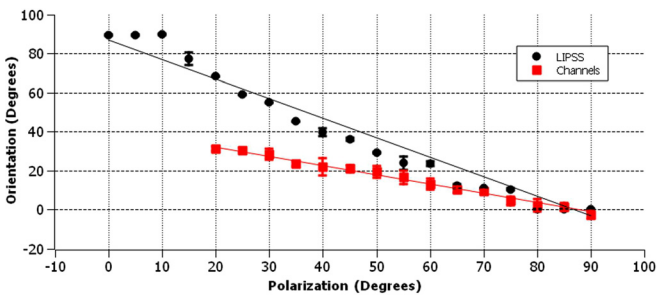

FIG. 4. Plot of LIPSSs and microgroove orientation with respect to the surface component of the laser's polarization.

As we see from this study, grooves formed from large incident angle ablation grow parallel to the plane of the laser beam's propagation direction for s-polarizations, but form at polarization-dependent angles for mixed polarizations, and interestingly do not form for p-polarizations. To understand this phenomenon, we must first discuss the formation of LIPSSs. First, defects present on the material's surface cause incident laser light to scatter electromagnetic waves along the material's surface. These scattered waves interfere with yet further laser irradiation and cause inhomogeneous and periodic absorption of the laser's energy.[24,25] In turn, this causes inhomogeneous and periodic ablation of the material, forming LIPSSs oriented perpendicular to the laser's polarization.

If the natural tendency of grooves is to form parallel to the laser beam's propagating direction, then periodic ablation, in the form of LIPSSs, occurs parallel to the forming grooves for s-polarized irradiation and perpendicular for p-polarization. In this way, mechanical groove growth is accentuated for s-polarized irradiation, forming a positive feedback effect between standard laser ablation and periodic ablation from LIPSSs, while being hindered for p-polarized irradiation due to negative feedback forming from LIPSSs occurring perpendicular to the direction of laser ablation. This formation mechanism—the positive (s-polarization) and negative (p-polarization) feedback effects of standard laser drilling and polarization-dependent periodic ablation due to scattered electromagnetic waves—explains why grooves are observed forming for s-polarizations but not for p-polarizations. We further hypothesize that these positive and negative feedback mechanisms are the root cause of the angled microgroove formation observed for mixed polarizations (Fig. 5).

B. Incident angle dependence

We propose that the angled microgroove structures we observe are formed primarily due to the large incident angle ablation and that LIPSS formation bias the forward ablation of grooves through either positive feedback (LIPSSs and laser ablation in parallel) or negative feedback (LIPSSs and laser ablation occurring orthogonally). To verify that large incident angle ablation is the cause of the long and shallow microgrooves observed, a study was conducted where the incident angle with respect to the target surface was varied in 10-degree steps from 0° to 60°. This study was performed using a pulse train of 15 000 pulses and repeated for three polarizations: s-polarization, 45-degree polarization, and

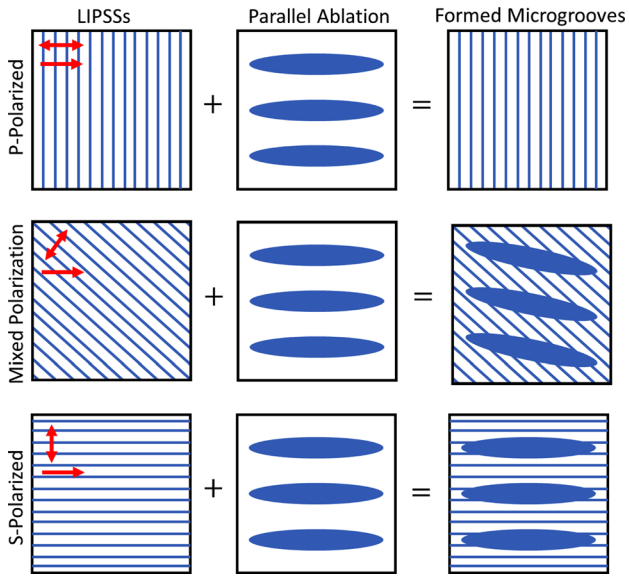

FIG. 5. Illustration of the proposed formation mechanism for observed microgroove formation. Polarization dependent LIPSS formation, forming simultaneously with ablation in the plane of the laser beam's propagation, cause formed microgrooves to orient at various angles or can inhibit microgroove growth entirely. The double headed arrow represents the laser beam's incident polarization, while the single headed arrow represents the laser beam's propagating direction.

p-polarization. Absorbed material fluence for this study was 4.99 mJ/cm^2. Careful attention was paid to maintaining consistent fluence due to polarization and incident-dependent absorptance and cross sectional area change.

From this study, it is clear that microgroove formation become elongated with a greater incident angle (Fig. 6). For normal and near-normal incident angle ablation, instead of forming microgrooves, a hole is drilled down into the Cu surface as is the case for standard laser drilling. For all incidence angles, no grooves were observed for p-polarized irradiation, instead axially symmetric wall markings are observed which congregate at, and fold in towards, the intensity maxima of the laser ablated area [Figs. 6(a)–6(c)]. Similar structures to Fig. 6(a) have previously been observed and are thought to be the result of self-organized structure formation.[29,30] For both 45-degree and s-polarized laser irradiation, structures formed with less than a 40° incident angle are non-uniform and without order [Figs. 6(d)–6(i)]. At incident angles above 40°, these structures grow in length, forming uniformly and with a singular orientation [Figs. 6(f) and 6(i)]. This study confirms that large incidence angle ablation is paramount to the formation of microgroove arrays. Without ablation of more than a 40° incident angle, grooves either do not form or form shallowly and non-uniformly. As the laser beam's incident angle increases, microgrooves formed grow in both length and uniformity.

C. Pulse number dependence

To validate our proposed formation mechanism—microgrooves formed from large incident angle ablation are biased by either positive feedback (LIPSSs and laser ablation in parallel) or negative feedback (LIPSSs and laser ablation

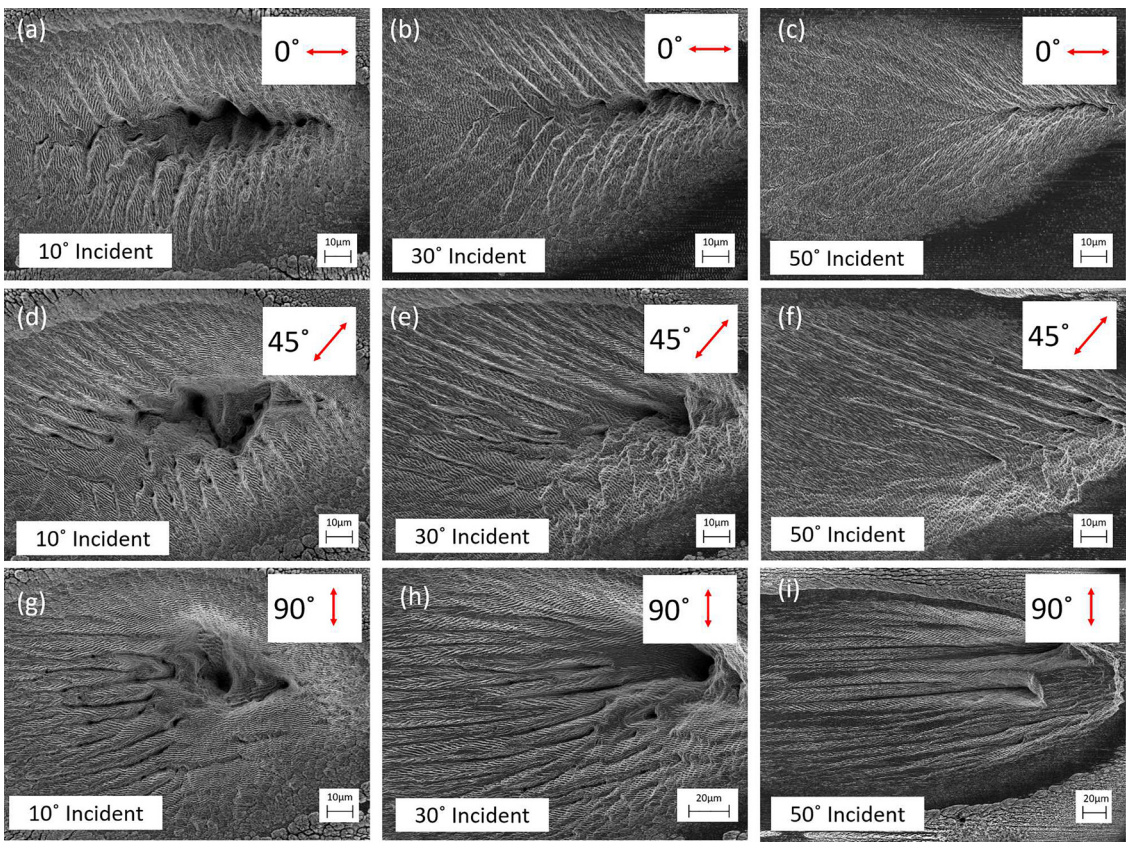

FIG. 6. SEM images of Cu irradiated by a femtosecond laser beam propagating towards the images right-hand side, with 15 000 pulses and at varied polarizations and incident angles.

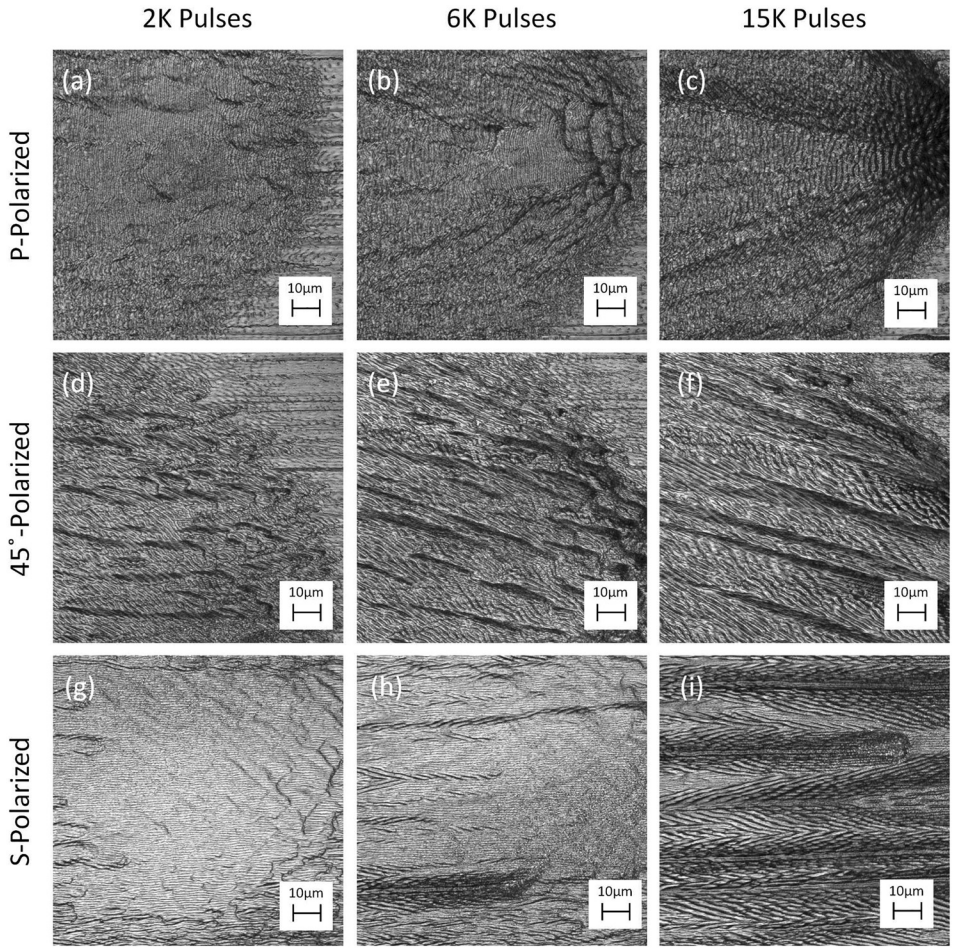

FIG. 7. Evolution of images of the same irradiated focal area for three polarizations, taken after successive pulse train bursts. Images were irradiated at a 50° incident angle, with the laser propagating towards the right-hand side of the image. The full set of images taken for this study can be seen in the multimedia view. Multimedia view: https://doi.org/10.1063/1.5028197.1

occurring orthogonally) mechanisms—we investigate the dynamics of microgroove growth by studying the shot-to-shot evolution that leads to the angled microgroove formation. To study the progression of these structures, images were taken of the same irradiated focal area between bursts of femtosecond pulses. This was accomplished by irradiating directly onto the stage of a confocal scanning laser microscope at a 50° incident angle. Figure 7 shows images taken after 2000, 6000, and 15 000 accumulated pulses; the full set of images taken for this study can be seen in the multimedia view of Fig. 7. An absorbed fluence value of 2.60 mJ/cm^2 was used for this experiment and, again, careful attention was paid to maintaining this fluence consistently across all polarizations.

For all polarizations, irradiating the Cu surface with 100–400 laser pulses produces an ablated area covered mostly in LIPSSs oriented perpendicular to the laser's polarizing direction. For p-polarized irradiation, as the pulse number is increased, LIPSS formation become hazy and no groove growth is observed [Figs. 7(a)–7(c)].

For s-polarized irradiation, microgrooves originate from defect spots on the Cu surface [Fig. 7(g)]. As the pulse number increases, these defects grow out in the direction of the laser beam's propagation [Figs. 7(h) and 7(i)]. This observation explains why instead of a single uniform laser ablated area, many grooves are formed. Defects upon the metal's surface ablate more readily than the surrounding area due to enhanced local absorption of the laser's energy, resulting in a multitude of microgroove formation. As the pulse number increases, formed microgrooves grow in length and uniformity, resulting in long parallel microgrooves.

For a polarization of 45-degrees, pulses up to 1k also create parallel ablation focused on defects. With continued laser pulses, these nascent microgrooves are observed altering their orientation towards the orientation of the LIPSSs that form uniformly along the material surface [Figs. 7(d)–7(f)]. This ablation does not occur at an angle but continuously parallel to the plane of the laser beam's propagation. This continuous parallel ablation is inhibited by LIPSS formation and shifts the focus of locally enhanced defect-focused ablation downwards; the result is an angled microgroove formation. This change in orientation stops around 10 000 pulses. A further increase in pulse trains no longer alters the forming groove's orientation and instead lengthens the grooves and shifts their overall position towards the laser beam's propagation direction.

The bow wave shaped sidewalls seen forming in Figs. 7(a)–7(c) are suggestive of material transport along the laser beam's propagation. Such structures indicate that hydrodynamics may play a role in the formation of the angled microgrooves we produce. Self-organizational models of structure formation have been shown to explain microgroove formation through hydrodynamic melt and resolidification processes,[31,32] and may explain the LIPSS mediated enhancement or inhibition of microgroove formation we observe.

LIPSSs are observed both inhibiting and accentuating the growth of microgrooves. For p-polarizations, LIPSSs form perpendicular to the plane of the laser beam's propagation, creating negative feedback and inhibiting microgroove growth [Fig. 7(c)]. For s-polarizations, LIPSSs form parallel to the plane of the laser beam's propagation, creating positive feedback and accentuating microgroove growth [Fig. 7(i)]. For 45-degree polarizations, LIPSSs forming at an angle to the laser beam's propagation exhibit both negative and positive feedback, inhibiting forward growth while enhancing growth in a particular direction [Fig. 7(f)]. These competing positive and negative feedback mechanisms result in grooves forming at a fixed bias angle roughly half that of the LIPSSs that bias their growth, as shown in Fig. 4.

IV. CONCLUSION

In conclusion, we have demonstrated the ability to form microgrooves with controllable orientation without translating or rotating the laser beam or sample. These microgrooves arise from femtosecond-pulsed irradiation and form as an array of grooves within a single laser spot. Microgrooves can be controlled between 0° and 30° with respect to the plane of the laser beam's propagation on the metal's surface and require an irradiating incident angle of at least 40°. A large incident angle is required to form the long and shallow microgrooves we wish to achieve, while the orientation of the microgrooves is due to feedback between continuous defect-focused laser ablation in the direction of the laser beam's propagation and polarization-dependent periodic ablation in the form of LIPSSs. LIPSSs forming perpendicular to the surface projection of the laser beam's propagation inhibit microgroove growth (negative feedback), while LIPSSs forming parallel to the surface projection of the laser beam's propagation accentuate microgroove growth (positive feedback). For mixed-polarizations, or off-angled LIPSSs, the combination of these two feedback mechanisms results in microgrooves forming at a fixed bias orientation.

ACKNOWLEDGMENTS

This work was funded by the Bill & Melinda Gates Foundation (OPP1119542) and the U.S. Army Research Office (W911NF-15–1-0319).

[1]R. Suriano, A. Kuznetsov, S. M. Eaton, R. Kiyan, G. Cerullo, R. Osellame, B. N. Chichkov, M. Levi, and S. Turri, Appl. Surf. Sci. **257**, 6243 (2011).
[2]J. P. McDonald, V. R. Mistry, K. E. Ray, and S. M. Yalisove, Appl. Phys. Lett. **88**, 183113 (2006).
[3]L. D. Stevanovic, R. A. Beaupre, A. V. Gowda, A. G. Pautsch, and S. A. Solovitz, in *Appl. Power Elect. Conference* (2010), pp. 1591–1597.
[4]U. Hermens, S. Kirner, C. Emonts, P. Comanns, E. Skoulas, A. Mimidis, H. Mescheder, K. Winands, J. Krger, E. Stratakis, and J. Bonse, Appl. Surf. Sci. **418**, 499 (2017).
[5]W. O. Soboyejo, B. Nemetski, S. Allameh, N. Marcantonio, C. Mercer, and J. Ricci, J. Biomed. Mater. Res. B **62**, 56 (2002).
[6]A. Fasasi, S. Mwenifumbo, N. Rahbar, J. Chen, M. Li, A. Beye, C. Arnold, and W. Soboyejo, Mater. Sci. Eng. C **29**, 5 (2009).
[7]B. N. Chichkov, C. Momma, S. Nolte, F. von Alvensleben, and A. Tünnermann, Appl. Phys. A **63**, 109 (1996).
[8]R. L. Harzic, N. Huot, E. Audouard, C. Jonin, P. Laporte, S. Valette, A. Fraczkiewicz, and R. Fortunier, Appl. Phys. Lett. **80**, 3886 (2002).
[9]R. R. Gattass and E. Mazur, Nat. Photonics **2**, 219 (2008).
[10]R. Osellame, H. Hoekstra, G. Cerullo, and M. Pollnau, Laser Photonics Rev. **5**, 442 (2011).
[11]S. Juodkazis, V. Mizeikis, and H. Misawa, J. Appl. Phys. **106**, 051101 (2009).
[12]A. Borowiec and H. Haugen, Appl. Phys. A **79**, 521 (2004).
[13]M. Shinoda, R. R. Gattass, and E. Mazur, J. Appl. Phys. **105**, 053102 (2009).
[14]A. Y. Vorobyev and C. Guo, Adv. Mech. Eng. **2**, 452749 (2010).
[15]A. K. Dubey and V. Yadava, Int. J. Mach. Tool Manufac. **48**, 609 (2008).
[16]H. Sezer, L. Li, M. Schmidt, A. Pinkerton, B. Anderson, and P. Williams, Int. J. Mach. Tool Manufac. **46**, 1972 (2006).
[17]C. McNally, J. Folkes, and I. Pashby, Mater. Sci. Technol. **20**, 805 (2004).
[18]J. F. Young, J. Preston, H. Van Driel, and J. Sipe, Phys. Rev. B **27**, 1155 (1983).
[19]A. Y. Vorobyev and C. Guo, Laser Photonics Rev. **7**, 385 (2013).
[20]T. Y. Hwang and C. Guo, J. Appl. Phys. **109**, 083521 (2011).
[21]B. Lam, J. Zhang, and C. Guo, Opt. Lett. **42**, 2870 (2017).
[22]J. D. Jackson, *Classical Electrodynamics*, 2nd ed. (John Wiley & Sons, Inc., 1962), pp. 219–220.
[23]S. Babar and J. Weaver, Appl. Opt. **54**, 477 (2015).
[24]J. Sipe, J. F. Young, J. Preston, and H. Van Driel, Phys. Rev. B **27**, 1141 (1983).
[25]J. Bonse, A. Rosenfeld, and J. Krüger, J. Appl. Phys. **106**, 104910 (2009).
[26]J. Wang and C. Guo, J. Appl. Phys. **102**, 053522 (2007).
[27]J. Bonse, S. Höhm, S. V. Kirner, A. Rosenfeld, and J. Krüger, IEEE J. Sel. Top. Quant. **23**, 9000615 (2017).
[28]P. Gregorčič, M. Sedlaček, B. Podgornik, and J. Reif, Appl. Surf. Sci. **387**, 698 (2016).
[29]O. Varlamova, M. Bounhalli, and J. Reif, Appl. Surf. Sci. **278**, 62 (2013).
[30]J. Reif, O. Varlamova, M. Ratzke, M. Schade, H. S. Leipner, and T. Arguirov, Appl. Phys. A **101**, 361 (2010).
[31]G. D. Tsibidis, C. Fotakis, and E. Stratakis, Phys. Rev. B **92**, 041405 (2015).
[32]G. D. Tsibidis, M. Barberoglou, P. A. Loukakos, E. Stratakis, and C. Fotakis, Phys. Rev. B **86**, 115316 (2012).